Summertime U.S. Precipitation Variability and Its Relation to Pacific Sea Surface Temperature

MINGFANG TING AND HUI WANG

Department of Atmospheric Sciences, University of Illinois at Urbana–Champaign, Urbana, Illinois

ABSTRACT

The year-to-year fluctuations in summertime precipitation over the U.S. Great Plains are examined in this study using data from 1950 to 1990. There are large interannual variabilities in precipitation amounts over the Great Plains during the period considered. A long-term trend in Great Plains precipitation from relatively wet conditions in the 1950s to relatively dry conditions in the 1980s is also identified. The spatial scale of the anomalous precipitation covers a large portion of the United States on seasonal mean timescales.

It is shown that the Great Plains precipitation fluctuations are significantly correlated with the tropical, as well as North Pacific, sea surface temperature (SST) variations. Two leading modes of covariation between Pacific SST and the U.S. precipitation are identified, with the first mode having spatial and temporal characteristics of the El Niño–La Niña SST variation, while the second mode is confined to the North Pacific and contains the decadal trend. The relationship of both the SST and the precipitation variation with the atmospheric circulation is established through 500-mb height, as well as the sea level pressure fields. A well-defined wave train over the Pacific and North American region is found to be associated with the two leading modes. A southward-shifted jet stream over the central United States brings more synoptic storms into the region and causes excessive precipitation during wet events. The tropical SST and the U.S. precipitation may be connected through the anomalous tropical convection and its effects on the circulation. The relation between North Pacific SST and the U.S. precipitation is consistent with a strong atmospheric forcing on the North Pacific SST at a 1-month lead. It is also hypothesized that North Pacific SST feeds back onto the circulation through an enhanced (reduced) Pacific jet due to the increase (decrease) of the meridional SST gradient during dry (wet) summers. This appears to be consistent with the enhanced convection along the Pacific storm track and the intensified Pacific jet stream in the two recent dry summers (1983 and 1988).

1. Introduction

The great flood in the summer of 1993 and the great drought in the spring and summer of 1988 raise serious questions about the causes of the warm season climatic fluctuations over the United States. Many efforts in the past years have been put into the understanding of the possible mechanisms for the 1988 drought. Both the atmospheric and the oceanic circulations were extremely anomalous during the spring and summer of 1988 (NOAA 1988). A strong La Niña condition over the tropical Pacific was under way, and at the same time, large sea surface temperature (SST) anomalies were also present over the North Pacific throughout the spring and summer of 1988. On the other hand, the North American landmass was dominated by an anticyclonic circulation anomaly in the upper troposphere, which persisted for several months in both the spring and summer of 1988.

Some effects of the anomalous tropical convection during the spring and early summer of 1988 have been discussed by Trenberth et al. (1988) and Trenberth and Branstator (1992). By specifying the anomalous soil moisture conditions, as well as the SST anomalies, in the Goddard Laboratory of Atmosphere general circulation model (GCM), Atlas et al. (1993) were able to reproduce many of the circulation anomalies for the 1988 drought. The physical and dynamic processes involved in the drought, however, are complicated. The interaction of the local circulation anomaly during the drought with the midlatitude storm track dynamics and that with the dry soil condition could both have been important for the maintenance of the 1988 drought (Mo et al. 1991; Namias 1991; Trenberth and Guillemot 1996).

In establishing the physical processes during the 1993 summer flood, Trenberth and Guillemot (1996) again linked the anomalous tropical convection due to the El Niño–related SST with the circulation anomalies over the United States. As in the 1988 drought, SST anomalies were present over both the tropical and the midlatitude Pacific throughout the summer season in 1993 (NOAA 1993). Other physical and dynamic pro-

Corresponding author address: Dr. Mingfang Ting, Dept. of Atmospheric Sciences, University of Illinois at Urbana–Champaign, 105 South Gregory Avenue, Urbana, IL 61801-3070.
E-mail: ting@atmos.uiuc.edu

cesses, such as the storm track changes, the low-level moisture transport, and the soil moisture feedback, each play an important role in the maintenance of the flood circulation (Mo et al. 1995; Trenberth and Guillemot 1996).

Although effects of the tropical SST anomalies on the 1988 drought and the 1993 flood have been emphasized by Trenberth and colleagues (Trenberth et al. 1988; Trenberth and Branstator 1992; Trenberth and Guillemot 1996), there is, however, little emphasis on the possible linkage between the North Pacific SST and the Great Plains precipitation fluctuations. Furthermore, the role of tropical and North Pacific SST anomalies in other drought and flood events (prior to the 1988 event) needs to be determined. It is thus useful to further study the relation of both the tropical and North Pacific SST anomalies with the precipitation fluctuations over the U.S. Great Plains for a long period of record. The following questions will be addressed. What are the typical SST patterns that accompany the drought and flood years over the Great Plains? Are there physical mechanisms that can link the SST anomalies with the Great Plains rainfall variations during summer?

The relationship between the tropical and North Pacific SST anomalies and the atmospheric circulation has been the subject of many observational and modeling studies in the past. Most of these studies were focused on the cold season. It is well recognized that the El Niño–La Niña SST anomalies exert a strong influence on the global atmospheric circulation in the winter (e.g., Horel and Wallace 1981) through Rossby wave dispersions (Hoskins and Karoly 1981). This conclusion is well confirmed using atmospheric GCMs with fixed tropical Pacific SST anomalies (e.g., Lau 1985; Blackmon et al. 1987; among others). Recent studies using both observations and a GCM (Held et al. 1989; Ting and Hoerling 1993; Hoerling and Ting 1994) show that the process may be complicated by the midlatitude transient feedback.

For the midlatitude, Wallace and Jiang (1987) found significant correlations between atmospheric circulation anomalies and the North Pacific SST anomalies. This correlation appears to be even stronger than the corresponding correlation between the extratropical atmospheric circulation and the tropical Pacific SST. Wallace et al. (1990) further confirmed the strong relationship between North Pacific SST and the atmospheric circulation using the principal component analysis technique and found a basinwide coherent SST anomaly pattern associated with the extratropical teleconnections. It is subject to debate whether the North Pacific SST anomalies during winter exert a strong impact on the extratropical atmospheric circulation. Davis (1976) showed that, on monthly and longer timescales, the observed connection between SST and sea level pressure in the North Pacific Ocean is primarily the result of the atmosphere driving the ocean. The GCM experiments with fixed midlatitude SST anomalies are found to be

very sensitive to the model physics and design (Ting 1991; Kushnir and Lau 1992; Peng et al. 1995, Kushnir and Held 1996). The coupled ocean–atmosphere model experiments (Alexander 1992a,b; Lau and Nath 1994) tend to show a strong forcing by the tropical Pacific SST on the generation of North Pacific SST anomalies through the bridging effect of the midlatitude atmosphere.

Much less attention has been given in the past years to the possible relation between *summertime* SST anomalies and the climatic fluctuations. Bunkers et al. (1996) found that the precipitation and surface temperature anomalies over North and South Dakota during El Niño–La Niña are significant for the April through October months. Namias (1983) computed the correlation between surface air temperatures averaged over the nine Great Plains states and the North Pacific SST for the summers of 1947 through 1980. He found a coherent pattern in the North Pacific, with positive correlations in the eastern North Pacific and negative correlations in the central Pacific. This led Namias to conjecture the possible effect of North Pacific SST anomalies on the Great Plains summer drought. Lanzante (1984) also confirmed such a pattern using rotated empirical orthogonal function analysis on the cross-correlation matrix of SST and 700-mb heights. These results tend to suggest a strong simultaneous correlation during the summer, similar to that during the winter, between North Pacific SST anomalies and the atmospheric circulation. Given the large socioeconomic impact of the severe drought and flood events in the summer, it is vitally important to further examine whether the precipitation fluctuations in the Great Plains are in any way caused by the coherent North Pacific SST fluctuations that are likely to recur in the future. Although observational data analysis alone may not be able to disclose the cause and effect relationship between the oceans and the atmosphere, understanding the observational links may lead to an improved ability for seasonal predictions of the Great Plains drought and flood potentials.

The present study focuses on the data analysis of the linkage between the Great Plains precipitation fluctuations and the North Pacific SST anomalies during the warm season. Data analysis is also performed on the 500-mb geopotential height field, in relation to both the North Pacific SST and the Great Plains precipitation. The data used in this study cover a more extended period than those contained in most of the previous studies. Various statistical techniques, including correlation analysis, composite analysis, and the singular value decomposition, are utilized to aid a systematic documentation of the relationship.

In the following section, observational datasets and statistical techniques are described, and this is followed by the presentation of analysis results in section 3. Some discussions are given in section 4, and conclusions are given in section 5.

2. Data and methods

a. Data

The basic datasets used in this study are the monthly mean precipitation over the United States, the global SST, and the Northern Hemisphere 500-mb geopotential height. All data are averaged over the three summer months—that is, June–August (JJA)—to obtain the summer seasonal mean values, after the subtraction of the long-term mean seasonal cycle.

The monthly mean U.S. precipitation is taken from the Global Historical Climatological Network (GHCN) from Oak Ridge National Laboratory. The GHCN database consists of station observations over land for the period 1851–1990. In this study, we only use data for the 41-yr period from 1950 to 1990. These station data were binned into regular 2.5° lat × 2.5° long grids by averaging over all the available stations within the grid box. All station data were quality controlled before further processing. The data coverage over the United States is reasonably good for the period considered. On average, there are about 8 to 10 stations within each 2.5° × 2.5° box. There are, however, potential problems with the precipitation dataset due to changes in measurement techniques and station locations over the years (Groisman and Legates 1994). These biases are found to be the largest for winter season and for mountainous regions, as well as for high latitudes. For the summertime U.S. precipitation considered in this study, the precipitation data are reasonable, except for the regions close to the Rockies.

The global SST is taken from Reynolds reconstruction of the Comprehensive Ocean–Atmosphere Data Set (COADS) SST, as described in Smith et al. (1996). The SST anomalies for the period 1950–92 were reconstructed based on the dominant empirical orthogonal function modes derived from a more recent period, 1982–93. This procedure helps to produce smoother SST fields than the traditional analyses, and the large-scale ENSO signal was enhanced through the improved interpolation. All SST data were computed on a 2° lat × 2° long COADS grid and from 45°S to 69°N.

The monthly mean 500-mb height data are obtained from National Centers for Environmental Prediction (NCEP) operational analyses. The height data are analyzed on a 2.5° lat × 5° long grid and cover the Northern Hemisphere poleward of 20°N. This dataset has known spurious trends for the period considered here, as discussed in Trenberth and Hurrell (1994). Thus, the correlation analysis carried out in this study may have suffered from this artificial trend. The use of an independent sea level pressure data helps to support the relationship identified using the 500-mb heights, however.

b. Analysis techniques

Several statistical approaches widely used in meteorological data analysis were taken in this study. The first is the simultaneous and lag/lead correlation between two chosen time series. This technique may suffer from having to subjectively choose a base time series. The subjectiveness of the correlation analysis is partially compensated for in the singular value decomposition (SVD) technique, which is very powerful in objectively detecting the coupled patterns between two fields. The SVD analysis yields two sets of spatial patterns and the associated time series by finding the eigenvalue solution of the temporal cross-covaraince matrix between the two fields. Each SVD mode consists of a pair of singular vectors together with the associated time series. The strength of the coupling between the two fields is measured by the amount of squared covariance explained by each mode and the temporal correlation coefficient between the two time series. The relative importance of the mode is determined by the fraction of the total variance explained by each mode. The detailed formulation of this analysis technique has been given by Bretherton et al. (1992) and applied by Wallace et al. (1992) who illustrated the coupled variability between wintertime North Pacific SST and 500-mb heights. Some caveats related to the SVD method are discussed in a recent paper by Newman and Sardeshmukh (1995).

3. Results

a. Precipitation variability over the United States

The JJA seasonal mean precipitation climatology is shown in Fig. 1a for the United States. On average, the amount of rainfall varies from about 6 mm day^{-1} over the southeast corner of the United States to less than 0.25 mm day^{-1} along the California coast. Large centers of precipitation in the summer are found along the Gulf of Mexico and the Mexican monsoon region. These decrease slowly toward the north and west. Local maxima are also found over the central plains bordering Kansas, Missouri, and Iowa. The rainfall amount in Fig. 1a may be underestimated due to gauge measurement biases (Groisman and Legates 1994). The large-scale spatial pattern, however, should be less affected.

Figure 1b illustrates the variability of summertime precipitation over the United States in the standard deviation of precipitation. Large fluctuations in seasonal mean rainfall amounts are found to coincide with regions of large total precipitation. Since precipitation is a positive definite quantity, the variability of the absolute amount of rainfall tends to be biased toward regions of large normal precipitation. A distinctive maximum is found in Fig. 1b, with 1.2 mm day^{-1} precipitation fluctuation over the central Plains, located on the border of Kansas and Missouri. Since this region is an area of major corn and soy bean production, it is of particular interest to understand this characteristic and the possible causes for the large precipitation fluctuations.

To examine the spatial coherence of the summer sea-

(a) PRCP Mean (mm/day) JJA 50-90
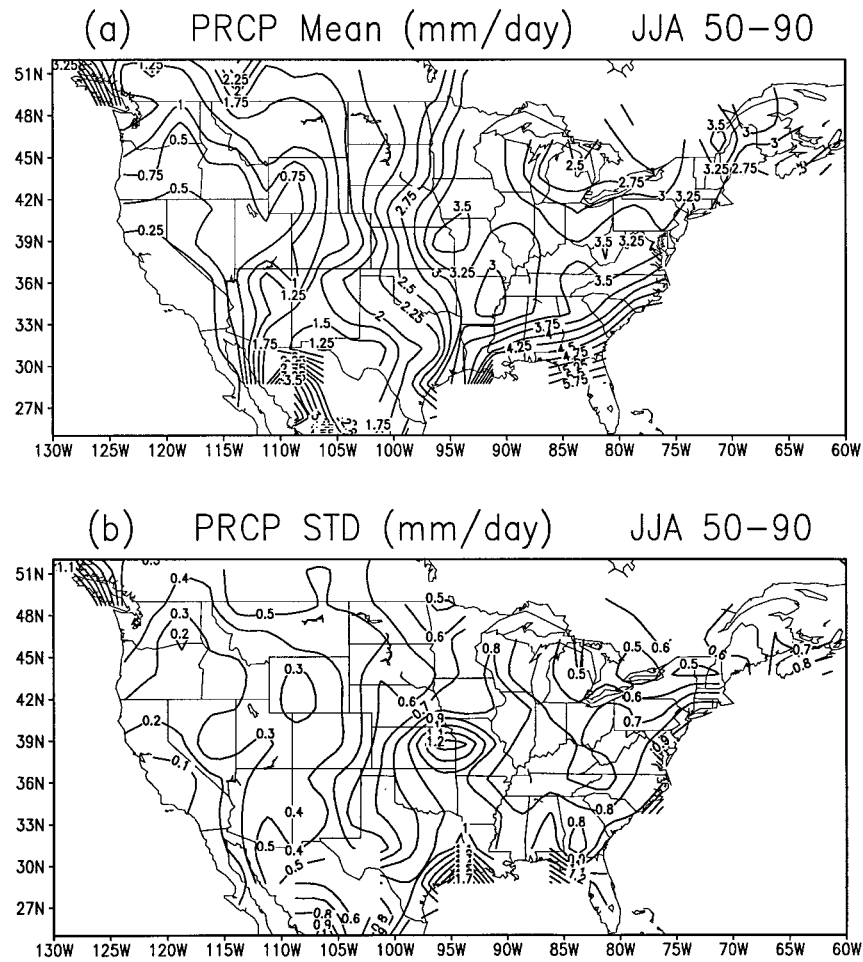

(b) PRCP STD (mm/day) JJA 50-90

FIG. 1. (a) Climatological mean and (b) standard deviation of summer seasonal mean precipitation over the continental United States for the period 1950–90. Contour intervals are (a) 0.25 mm day^{-1} and (b) 0.1 mm day^{-1}.

sonal mean precipitation fluctuations over the central plains, we computed the simultaneous correlation of the precipitation time series at the location of the maximum standard deviation, about 96°W and 39°N, with the rest of the grids over the United States. Such a one-point correlation map is shown in Fig. 2. The correlation at the base grid is equal to 1, and it gradually decreases away from the base grid. The one-point correlation shows significant values over a broad region extending from 33° to 43°N and 105° to 85°W. The region of significant correlation tilts northwestward in a band covering a large part of Wyoming and Montana. Significant negative correlations are noticeable over the Pacific Northwest states and southern Canada. Figure 2 suggests that the spatial scale of precipitation anomalies over the United States is rather large on seasonal mean timescales. A typical climate model of grid size on the order of 2° lat × 3° long (e.g., R30) should be able to adequately resolve these anomalies.

To examine the year-to-year fluctuations of the Great Plains precipitation, we constructed an area-averaged precipitation time series based on the scale shown in Fig. 2. The precipitation index time series, after averaging over all grids from 85° to 105°W and 32.5° to 45°N and being normalized by its standard deviation, is shown in Fig. 3. During the 1950s, there were large precipitation fluctuations over this region, with two extremely wet summers followed by five relatively dry summers. After one summer with close to normal precipitation in 1957, the summer of 1958 marked more extremely wet conditions across the Great Plains. During the 1960s and the first half of the 1970s, there were relatively small fluctuations in precipitation. The summer of 1976 marked the beginning of another period with large year-to-year variations in precipitation, which continued through the 1980s. The summers of 1976, 1983, and 1988 were the driest within this period according to this index, while the summers of 1950, 1951, and 1958 were the wettest. There is a slight trend in Fig. 3, with wetter conditions in the early period and relatively dry conditions in the later years. This trend is also reflected in that all three extremely wet summers
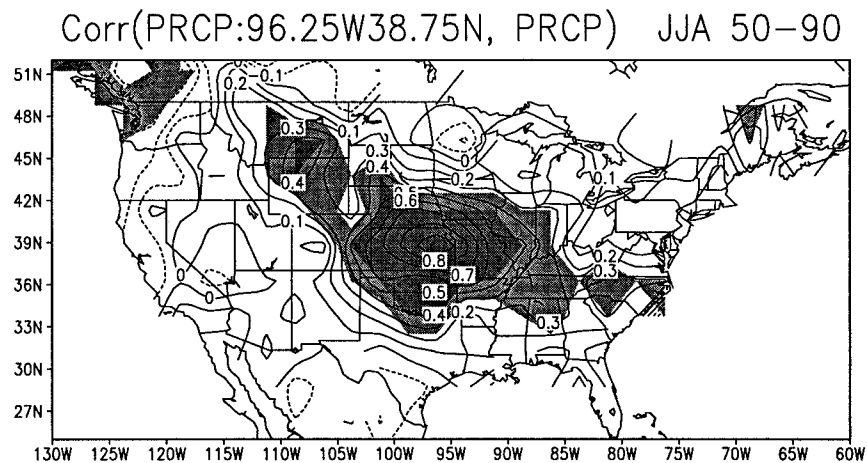
FIG. 2. One-point correlation of summer seasonal mean precipitation over the United States using the base grid at 38.75°N and 96.25°W, which is close to the maximum precipitation standard deviation in Fig. 1. Contour interval is 0.1, and negative contours are dashed. Those values exceeding the 5% Monte Carlo statistical significance level are in light shading, and those exceeding the 1% significance are in dark shading.

were in the 1950s, while the three driest summers are all found after 1976. The heat wave of 1980 has been discussed previously in the literature (Namias 1982; Chang and Wallace 1987; Lyons and Dole 1995). The anomalous precipitation during 1980 did exceed one standard deviation in the precipitation index (Fig. 3), but it is not as severe as the three dry years listed above.

Figure 4 illustrates the distribution of precipitation anomalies for the three wettest and the three driest summers discussed above. The anomaly patterns in Fig. 4 vary from case to case. But in almost all cases, there is

a coherent anomaly across the central and eastern United States east of 105°W. The amplitude of the anomaly in Fig. 4 is biased toward the wet events, again reflecting the nonnegative nature of the precipitation.

b. Relation between SST and precipitation

Given the relationship between 1988 SST and the Great Plains drought, we examine the SST anomalies associated with the three wettest and the three driest summers of Fig. 4 in Figs. 5a–f. Notice that while the
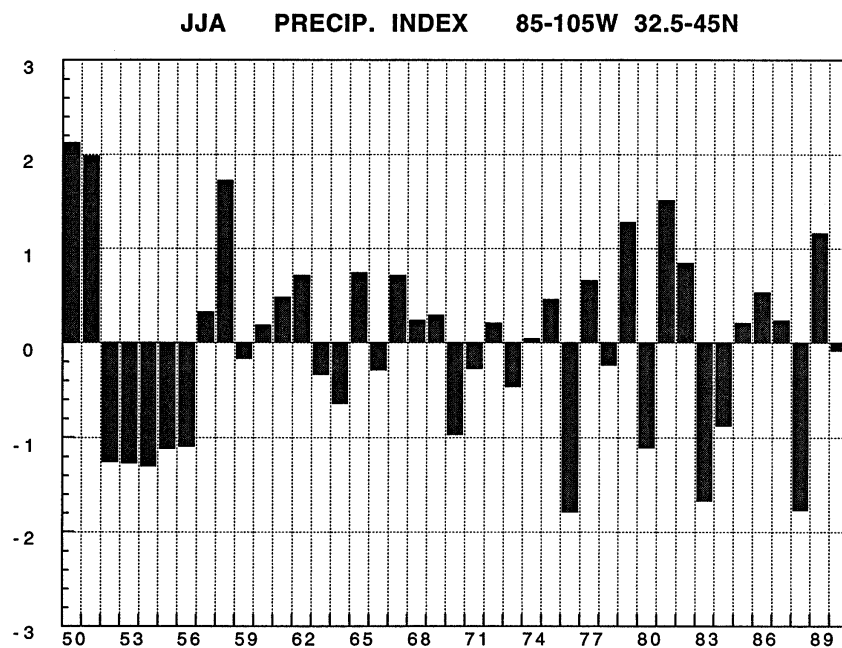

FIG. 3. Normalized precipitation time series averaged over the Great Plains from 105° to 85°W and 32.5° to 45°N. Units are in standard deviations.
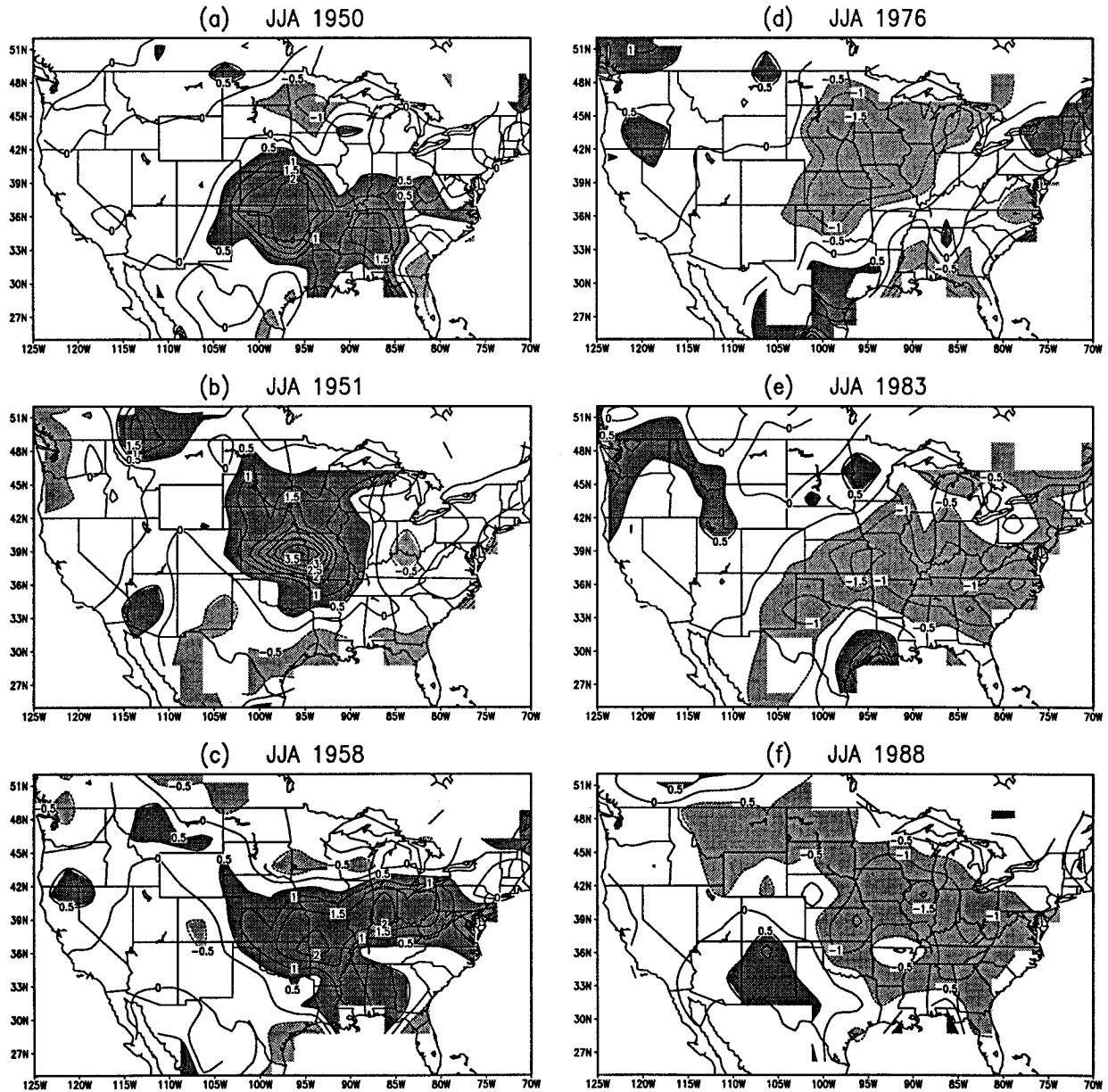
Precipitation Anomaly

FIG. 4. Anomalous precipitation over the United States for (a) JJA 1950, (b) JJA 1951, (c) JJA 1958, (d) JJA 1976, (e) JJA 1983, and (f) JJA 1988. Contour interval is 0.5 mm day^{-1}, and negative contours are dashed. Values greater than 0.5 mm day^{-1} are in dark shading and those less than -0.5 mm day^{-1} are in light shading.

tropical Pacific SST varies greatly from one case to another, the midlatitude SST anomalies seem to recur for almost all cases, with above-normal (below normal) eastern and western Pacific SST and, to a lesser degree, the cold (warm) central North Pacific SST associated with the wet (dry) pattern in Fig. 4.

To further examine the general relationship between SST and the U.S. precipitation, we calculated the simultaneous correlation of the precipitation index in Fig.

3 with the global SST. The correlation coefficient is shown for the Pacific north of 20°S in Fig. 6, where large areas of significant correlation were found. The light and dark shadings in Fig. 6 indicate the Monte Carlo statistical significance at the 5% and 1% levels, respectively. Significant correlations are found over the eastern and central North Pacific, as well as over the tropical Pacific. The pattern of correlation over the North Pacific is consistent with Namias (1983), who
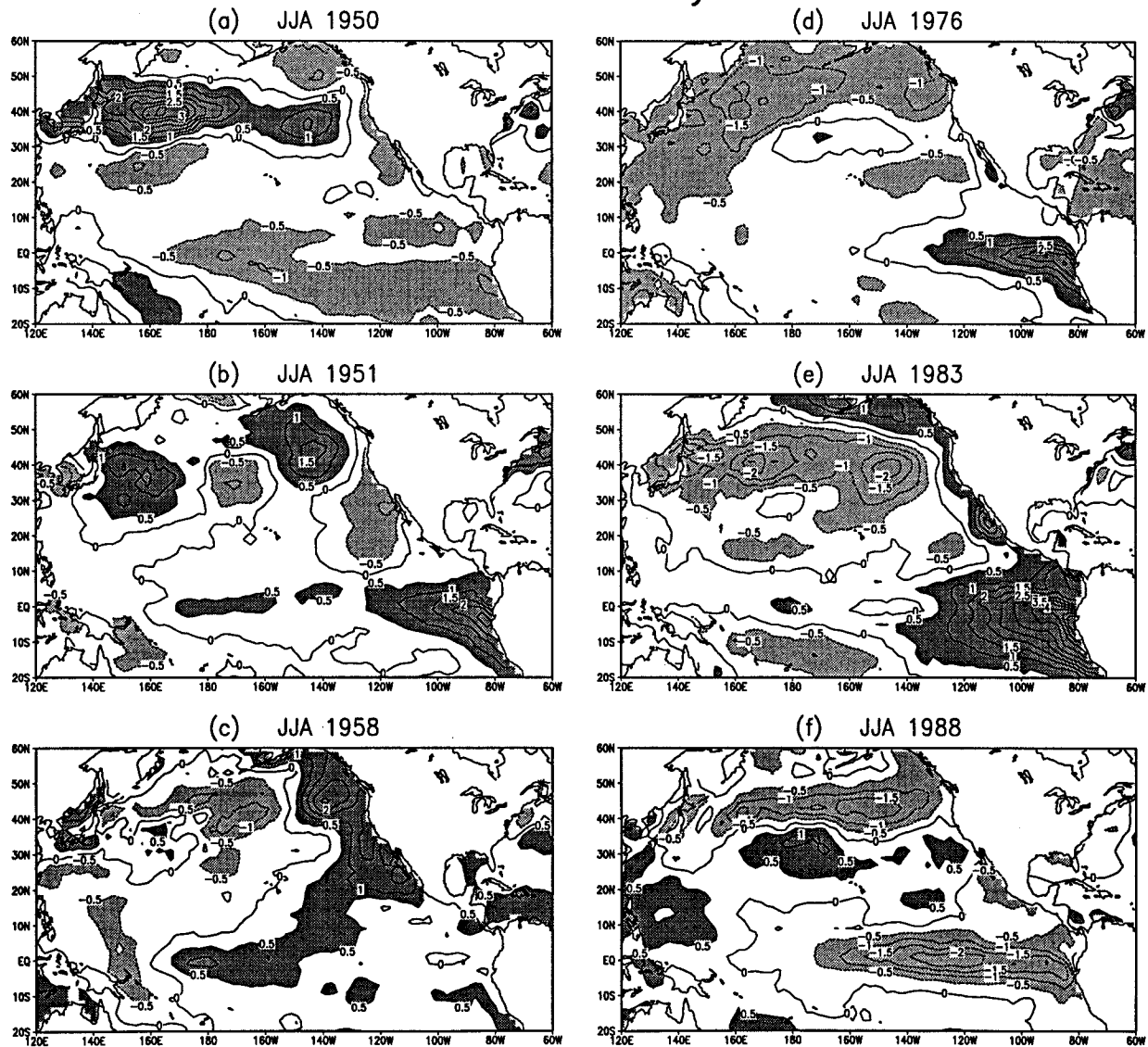
SST Anomaly

FIG. 5. Same as Fig. 4 but for the Pacific SST anomalies. Contour interval is 0.5°C, and negative contours are dashed. Dark shading is for values greater than 0.5°C, and light shading for those less than −0.5°C.

computed the correlation between SST in the North Pacific and the surface air temperatures over the Great Plains for the summers of 1947–80. Walsh and Richman (1981) also found a similar correlation pattern when the North Pacific SST is correlated with the first rotated empirical orthogonal function of the U.S. surface air temperatures, consistent with the fact that summer precipitation and the surface air temperature are negatively correlated over much of the Great Plains (Namias 1983; Zhao and Khalil 1993; Madden and Williams 1978). The correlation between the precipitation index and the tropical Pacific SST, while significant, is relatively small compared with the correlation over the midlatitudes. This is consistent with the impression gained from Fig. 5.

One potential caveat of the correlation analysis is the dependence of the correlation pattern in Fig. 6 on the subjectively chosen precipitation index time series. To further confirm the correlation results in Fig. 6, we performed singular value decomposition between the Pacific SST north of 20°S and the U.S. precipitation. The first two singular modes are shown in Fig. 7 in heterogeneous correlation maps. The heterogeneous correlation illustrates the spatial pattern of SST (precipitation) that is coupled to the time fluctuation of the U.S. precipitation (Pacific SST). The squared covariances explained by these modes are 33.8% and 21.0%, respectively. The first mode (Fig. 7a) clearly illustrates a tropical Pacific SST pattern that is typical of El Niño–La
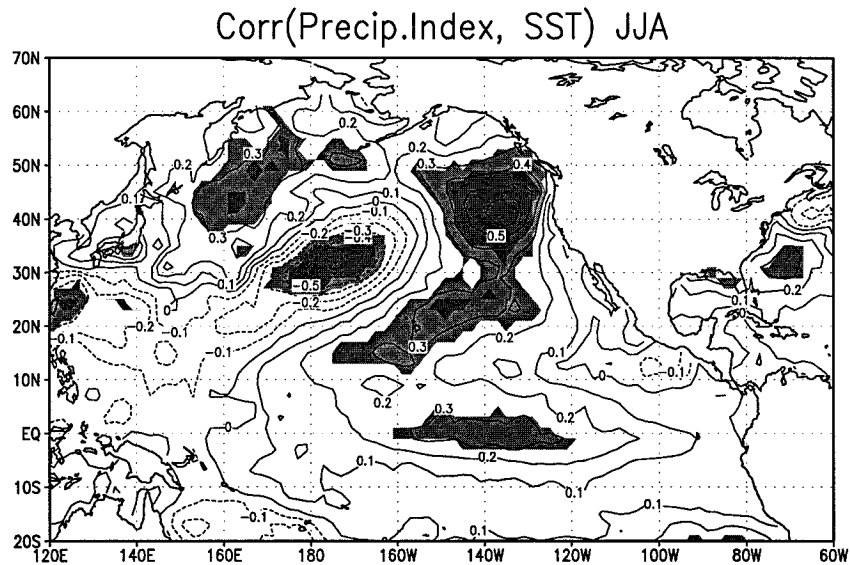
Corr(Precip.Index, SST) JJA

FIG. 6. Correlation coefficient of the precipitation index in Fig. 3 with the sea surface temperature for the summers of 1950 through 1990. Contour interval is 0.1, and negative values are dashed. Those values exceeding the 5% Monte Carlo statistical significance level are in light shading, and those exceeding the 1% significance are in dark shading.

Niña conditions. A warm tropical Pacific is coupled with relatively cold water over the central North Pacific and warm water farther north. The associated precipitation pattern (Fig. 7b) shows above-normal precipitation over the northern Great Plains and below-normal precipitation over the southeastern part of the United States. The SST pattern shown in Fig. 7a explains 29.0% of the total SST variance over the Pacific, whereas the precipitation pattern in Fig. 7b explains 7.0% of the total U.S. precipitation variance. The second mode of SST (Fig. 7c) very closely resembles the correlation pattern shown in Fig. 6 north of 20°N, with a positive center in the eastern and western North Pacific and a negative center in the central North Pacific. In the Tropics, however, there is very little amplitude in Fig. 7c. This mode explains 13.7% of the total SST variance. The associated precipitation pattern (Fig. 7d) has a large amplitude extending from 105°W to the East Coast and explains 10.3% of the total U.S. precipitation variance.

The precipitation index in Fig. 3 contains a signal associated with both the tropical and extratropical SST variabilities. The tropical SST tends to be more related to precipitation over the northern part of the Great Plains, centered over Wyoming and Nebraska, whereas the extratropical SST is more related to the central and eastern U.S. precipitation. Although the correlation in Fig. 7d is slightly less significant than that in Fig. 7b, the precipitation variance (10.3%) explained by the second mode is larger than that of the first mode (7.0%). The results in Fig. 7 evidently separate the tropical and extratropical SST modes, which are both coupled with the U.S. precipitation fluctuations. Deser and Blackmon (1995) performed a similar analysis, which

separates the tropical and extratropical SST variations for the winter season using an empirical orthogonal function method.

The time series associated with each mode and each variable are shown in Fig. 8. The first SST mode shows a year-to-year fluctuation (Fig. 8a), with above- (below) normal coefficients corresponding to well-known El Niño (La Niña) events. For example, the summer of 1987 was a strong El Niño event, whereas 1988 was a well-known La Niña. In general, above- (below) normal tropical Pacific SST is associated with above- (below) normal precipitation over the northwestern Great Plains (Fig. 8b). A recent study by Bunkers et al. (1996) found the April through October rainfall anomalies over the Dakotas are significantly above normal during El Niño years and below normal during La Niña years. From Fig. 7b, significant correlations are found over the southwestern portion of North Dakoda and a large part of South Dakota, thus confirming the finding in Bunkers et al. (1996). This tropical Pacific SST–northern Great Plains rainfall relationship was strong for the 1988 La Niña and, to a lesser extent, for the 1987 El Niño (compare Figs. 8a and 8b). The correlation between the two time series in Figs. 8a and 8b is 0.70. The SST time series for the second mode (Fig. 8c) shows very different behavior than the first mode. There is a clear trend over this period from above-normal coefficients in the 1950s and 1960s, which corresponds to a warm eastern and western North Pacific and a cold central North Pacific, to below-normal values in the late half of 1970s and 1980s. Such decade-long North Pacific SST variation and its relation to tropical Pacific SST during northern winter has been studied by Trenberth and Hurrell (1994)
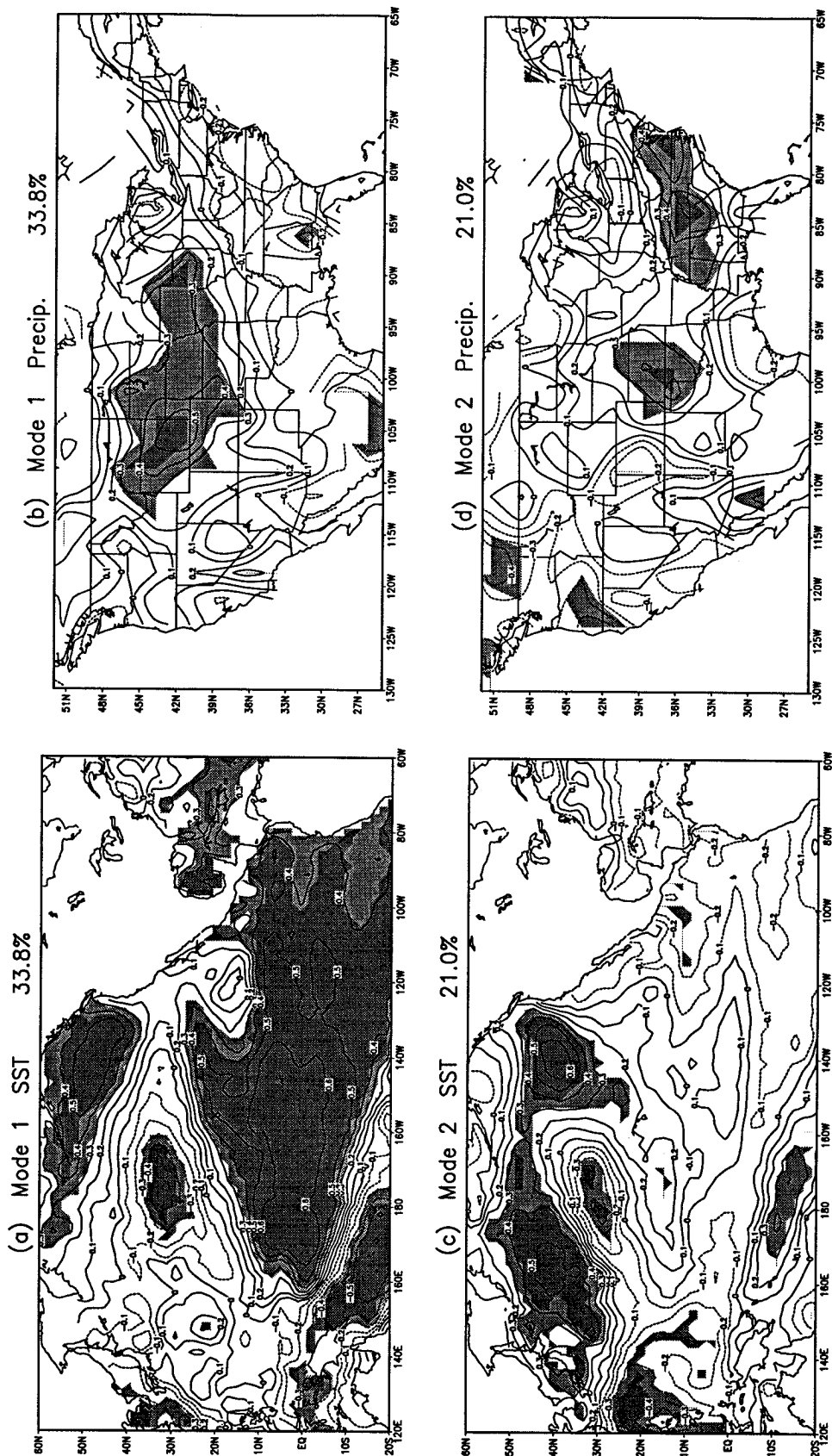
SVD: SST vs Precip.

FIG. 7. The leading two SVD modes in heterogeneous correlation for (a) SST mode 1, (b) precipitation mode 1, (c) SST mode 2, and (d) precipitation mode 2. Shadings are the same as in Fig. 6.
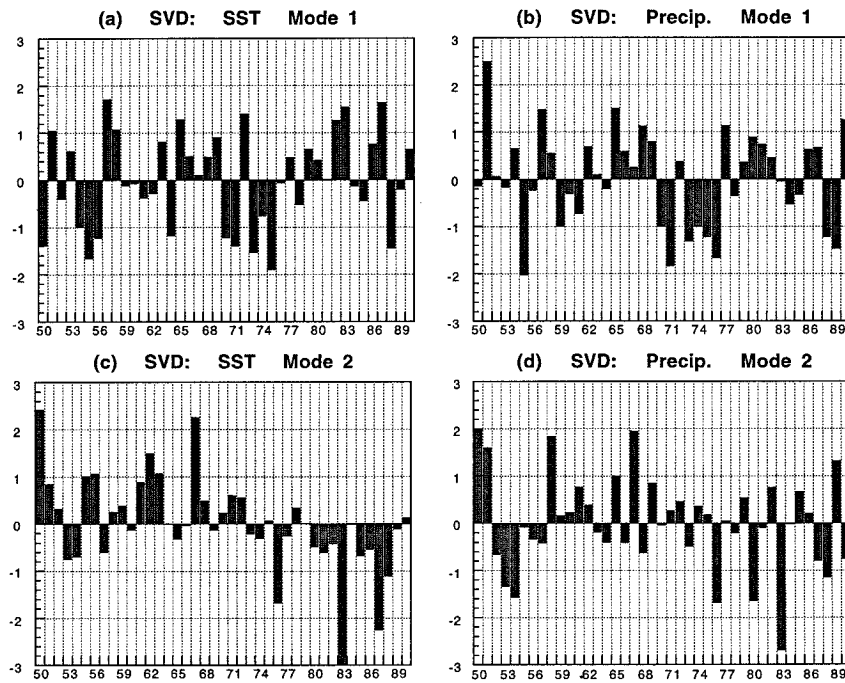
FIG. 8. The time series for the two leading SVD modes for (a) SST mode 1, (b) precipitation mode 1, (c) SST mode 2, and (d) precipitation mode 2. All units are in standard deviations.

and Graham et al. (1994), among others. The mechanism for the long-term variation in North Pacific SST is beyond the scope of this study. Our result here shows consistency of the summertime North Pacific SST variation with its winter counterpart (e.g., Deser and Blackmon 1995). The corresponding precipitation time series (Fig. 8d) shows more interannual fluctuations than the corresponding SST, although a similar decadal trend to that in Fig. 8c is also discernible. The long-term trend in Fig. 8d suggests that the slight decadal trend noted in the precipitation index in Fig. 3 may be related to the decadal variabilities of the North Pacific SST. The correlation between the time series shown in Figs. 8c and 8d is 0.66.

Note that the SST anomaly in 1988 (Fig. 4f) projects strongly onto both the tropical and the North Pacific modes, with negative coefficients. Thus, the precipitation anomalies related to the tropical and North Pacific SSTs add together in producing the drought condition over the Great Plains. On the other hand, the 1987 El Niño projects to the warm phase of the tropical Pacific mode, but negatively to the North Pacific mode (Fig. 8c). The resulting precipitation from the tropical mode and that from the North Pacific mode SST for 1987 tend to cancel each other. While the 1988 summer was an extremely dry one, 1987 was near normal. For the 1983 summer drought (Fig. 4c), the SST anomaly projects extremely (more than three standard deviations) onto the extratropical mode in negative phase. Even though

the SST in 1983 projects onto the warm phase of the tropical mode, the precipitation was below normal. Thus, different combinations of the effect of the tropical and the extratropical SSTs may contribute to the uniqueness of each of the drought or flood events.

The different nature of the tropical and the extratropical modes in Fig. 7 can be shown more clearly using the lead/lag heterogeneous correlations. In obtaining the lead/lag heterogeneous correlation, we correlate the precipitation time series in Fig. 8 with the Pacific SST of seasons leading and lagging the summer. For example, Figs. 9a–d show the heterogeneous correlation of the first SVD mode of precipitation with SST of the previous winter and spring seasons, as well as the following autumn and winter seasons, respectively. The tropical Pacific SST associated with the first SVD mode of precipitation has been undergoing an ENSO cycle, which initiates in the spring (Fig. 9b) and matures in the two seasons following the summer (Figs. 9c,d). The 1988 drought is a typical example of this case. On the other hand, the second mode is weakly related to the tropical Pacific SST of the previous winter (Fig. 9e). In the spring (Fig. 9f), the summer precipitation is showing significant correlation with the North Pacific SST, as well as the tropical Pacific SST. The North Pacific correlation with the second mode of precipitation reaches a maximum in the summer (Fig. 7c) and gradually diminishes in the fall (Fig. 9g) and winter (Fig. 9h). Thus, the second mode is more confined to the midla-

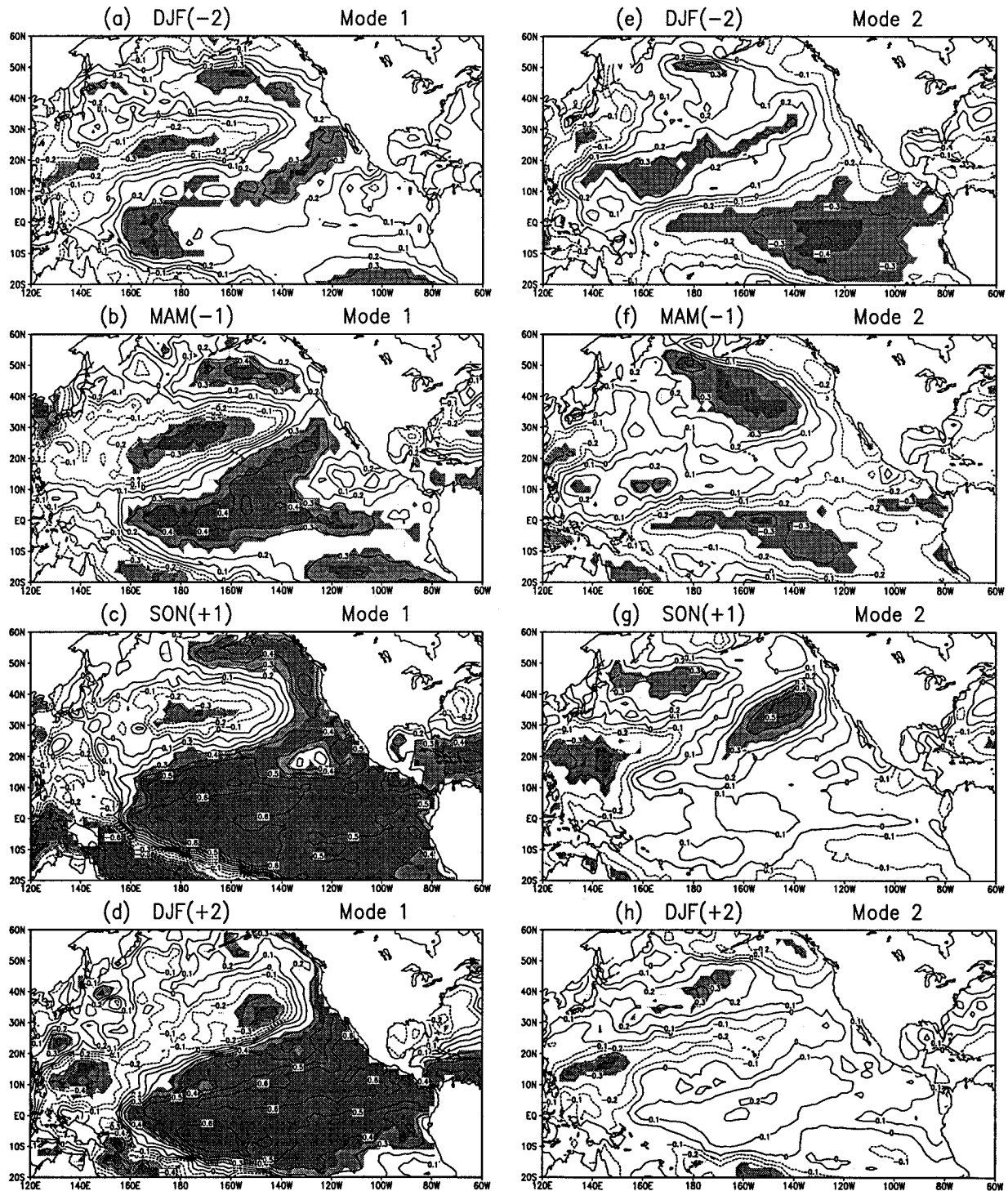## Lag/Lead Correlation of SST with Precip. SVD

FIG. 9. Lag and lead correlation between mode 1 SVD precipitation time series and the SST of (a) the previous winter, (b) the previous spring, (c) the following fall, and (d) the following winter, and between mode 2 SVD precipitation time series and the SST of (e) the previous winter, (f) the previous spring, (g) the following fall, and (h) the following winter. Contour interval is 0.1, and the negative contours are dashed. Shadings are the same as in Fig. 6.

titude Pacific, and it may be weakly forced by the tropical Pacific of the previous winter. The 1983 summer is a typical example of the second mode, when the 1982–83 strong El Niño ended in the winter and large North Pacific SST anomalies developed in the following spring and summer.

The connection between summertime precipitation and the springtime SST for both modes (Figs. 9b,f) raises the question of possible preconditioning of soil moisture in the spring. Although more detailed analysis using the available soil moisture data is necessary, preliminary calculations of the correlation between springtime precipitation and the precipitation of the following summer (not shown) did not show any significant correlation. Case studies of the time evolution of the 1988 and the 1983 droughts may shed some light on this issue and need to be pursued in the future.

c. Relation with atmospheric circulation

To examine the atmospheric circulation anomalies associated with both the U.S. precipitation and the Pacific SST anomalies during summer, we first computed the simultaneous correlation between the 500-mb heights at each grid point and the SVD time series shown in Fig. 8 (see Fig. 10). Statistically significant correlations are found in all four cases. For the first SVD mode, both the SST and the precipitation fluctuations are related to a wave train over the Pacific–North American (PNA) region. A negative center is found over the central North Pacific at 40°N, a positive center over the Gulf of Alaska, and another negative center over Hudson Bay in Fig. 10a. The correlation between height and precipitation (Fig. 10b) is somewhat stronger than that in Fig. 10a. In both cases, the correlation is significant in the subtropical band, indicating a possible tropical origin of this wave train.

The correlation of 500-mb heights with the second SVD mode is somewhat different from the first mode. The large centers in both the SST (Fig. 10c) and the precipitation (Fig. 10d) correlation are shifted southward from the corresponding position for the first mode. The negative correlation center in Fig. 10c over the North Pacific is located at 30°N, 170°W, about 10° south and slightly east of the corresponding center in Fig. 10a. The positive center along the west coast of North America has been shifted to the U.S. Pacific Northwest, and the negative center over the continent is located just southwest of the Great Lakes. The anomaly location is similar in Fig. 10d, but with almost doubled magnitude over the North American region. The maximum positive correlation along the coast is over 0.6, and the negative correlation over the United States is over 0.7 in Fig. 10d. The larger correlation between height and precipitation in Fig. 10d compared with that in Fig. 10c indicates a more direct control of the atmospheric circulation over the amount of rain falling in the region. An examination of the relative location of the height

anomaly (Figs. 10b,d) and the precipitation patterns (Figs. 7b,d) reveals that a low pressure center at 500 mb tends to be located slightly north of the region of excessive rainfall over North America.

To further examine the circulation features during dry and wet summers, we composited the three wet and the three dry summers shown in Fig. 4 to obtain the circulation characteristics during floods and droughts. The 500-mb geostrophic wind vectors calculated from the 500-mb height for the wet and dry composites are shown in Figs. 11a and 11b, respectively, along with the magnitude of the wind. The wind vector for the two SVD modes can be examined separately. We find that the main features are the same for both modes, but with the subtropical jet over the United States being shifted farther south for the second mode. Due to limited data samples, the composites are shown only for the combination of these two modes, based on the precipitation index shown in Fig. 3. The most distinctive difference between Figs. 11a and 11b is the southward-shifted and intensified jet over the North American region in wet summers, consistent with Fig. 10. The jet is significantly reduced and lifted farther north during dry years. The intensification of the jet during wet years over North America can be seen more clearly in the difference map (Fig. 11c). One also notices a strong northerly flow from inner Canada toward the western and central United States. Another noticeable feature in Fig. 11c is the reduced Pacific jet from the east coast of Asia all the way to the North American coast.

The relation between circulation at the surface and the SST and precipitation variability can be examined using the sea level pressure data. Figure 12 shows the correlation coefficients between sea level pressure north of 20°N and the time series of the SVD modes shown in Fig. 8. Although significant correlation is clearly present for all cases in Fig. 8, it is much weaker than the correlation between 500-mb height and the corresponding SST and precipitation time series. Almost all of the main centers at the surface have been shifted farther to the east relative to 500 mb, indicating a westward tilt of the anomalies. The negative center over the United States associated with wet summers (warm SST) is much less well defined at the surface than that at 500 mb. Figure 12 suggests that the surface signatures of the drought and flood may be much smaller than those aloft. The relation between the upper- and lower-atmospheric circulation anomalies associated with precipitation anomalies is worth of further investigation, as longer periods of the NCEP reanalyses data (Kalnay et al. 1996) become available in the future.

4. Discussion

The previous section shows evidence of a link between U.S. precipitation, the tropical and North Pacific SST, and the atmospheric circulation during summer. The physical mechanism underlying the linkage cannot
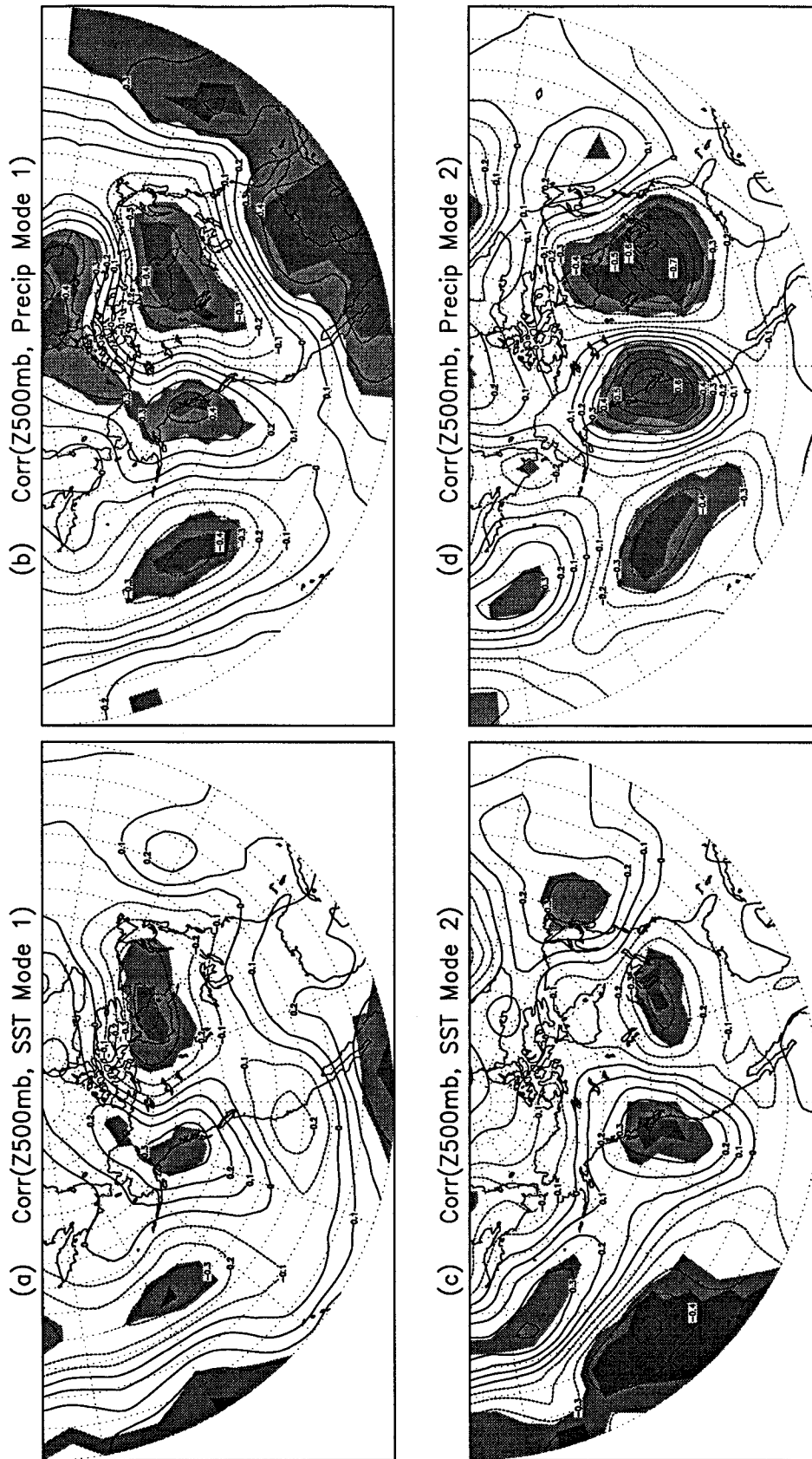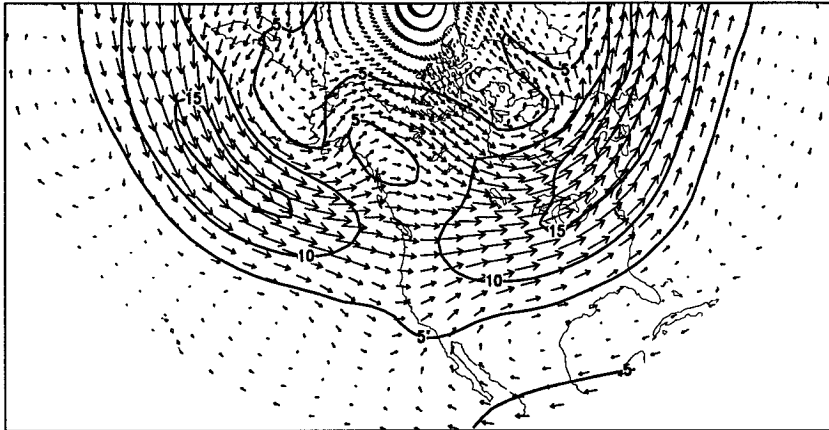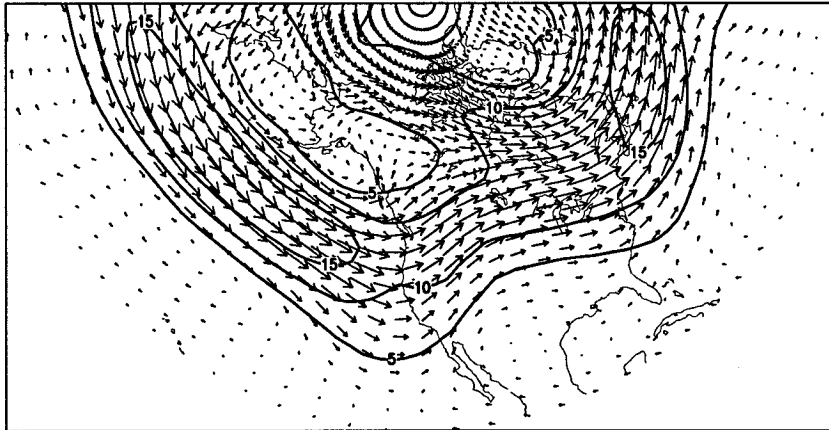
FIG. 10. Correlation coefficient of 500-mb heights with (a) mode 1 SST time series, (b) mode 1 precipitation time series, (c) mode 2 SST time series, and (d) mode 2 precipitation time series. Contour interval is 0.1, and negative contours are dashed. Shadings are the same as in Fig. 6.
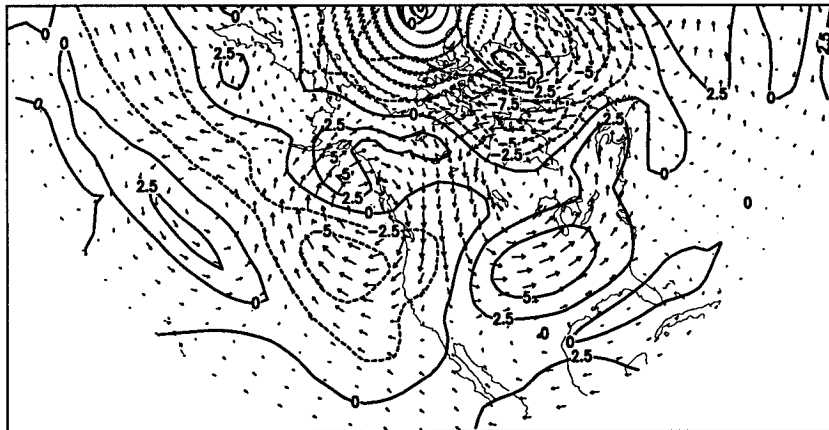
(a) Corr(Z500mb, SST Mode 1)

(b) Corr(Z500mb, Precip Mode 1)

(c) Corr(Z500mb, SST Mode 2)

(d) Corr(Z500mb, Precip Mode 2)

500mb Wind Composite

(a) Wet Years

(b) Dry Years

(c) Wet − Dry

$\overrightarrow{20}$

be established fully through observational analysis alone. The observational results, however, offer some suggestions for a possible explanation of the relationship.

a. Mechanisms of precipitation anomalies over the United States

Above- (below) normal precipitation over the United States is often associated with excessive (reduced) low-level moisture transport and frequent (less frequent) storm activities passing through the United States (e.g., Trenberth and Guillemot 1996; Mo et al. 1995). The linkage between North Pacific SST and the U.S. precipitation cannot be caused by direct moisture transport from the Pacific toward the U.S. land region, due to the presence of the Rockies and other mountain ranges in the western United States. Thus, the North Pacific SST can only be linked to the central and eastern U.S. precipitation through the change of atmospheric circulation over the United States, which leads to changes in moisture transport. As shown in Trenberth and Guillemot (1996), when vertically integrated total moisture flux is considered, the difference in moisture transport from the Gulf of Mexico between the 1988 drought and the 1993 floods is apparent. Due to the lack of a long period of data, a similar total moisture transport calculation cannot be performed in this case. With the reanalyses project at NCEP (Kalnay et al. 1996), more complete atmospheric data will become available, and a detailed study of the moisture transport for the dry and wet years can be carried out in the future. This will help determine the most important (lack of) moisture source during flood (drought) years.

The anomalous storm activity during 1993 has been shown to play a major role in producing the excessive rain for the summer (Mo et al. 1995; Trenberth and Guillemot 1996). Many previous studies have shown that storm tracks are organized largely by the time mean flow (Lau 1988; Branstator 1995; among others). The wind vector composites shown in Fig. 11 suggest a southward-shifted and enhanced storm track for the wet years and a northward-shifted and reduced storm activity in dry years over the U.S. region. With a large trough located over the North American land area, as indicated by the correlation in Fig. 10, there is a stronger northerly flow from interior Canada toward the United States. Combined with the southward-shifted storm track, this brings the atmospheric circulation during wet year summers into springlike conditions. When abundant moisture is available, this can easily develop into a flood event. The opposite is true for the dry years. If the jet

stream were located farther north and east and the mean 500-mb trough were located along the east coast of North America (Fig. 11b), storm activity would shift eastward and deviate more toward the Atlantic. If this condition were combined with the lack of a moisture source for the United States, a drought would result.

b. Relation between SST and atmospheric circulation pattern

The relation between U.S. precipitation and North Pacific SST is consistent with the notion that the North Pacific SST may be forced by the same atmospheric circulation pattern that causes rainfall anomalies. The strong atmospheric forcing on the North Pacific SST has been discussed by Davis (1976) using lag and lead correlations. The recent success of the North Pacific mixed layer ocean model in generating realistic SST variability when coupled to the global atmospheric GCM (Alxander 1992a; Lau and Nath 1994) further confirms the importance of atmospheric forcing on the midlatitude SST. To test this idea, we performed lag/lead correlation analysis using monthly mean SST and the 500-mb height fields. We first performed SVD analysis between Pacific SST and U.S. precipitation using the summer *monthly* mean data instead of the *seasonal* mean as shown in Fig. 7. The two leading SVD modes are essentially the same as in Fig. 7, but the order of the first and the second modes is switched. The first SVD mode based on the monthly mean data is the North Pacific mode, with a spatial pattern almost identical to that of the second mode in Figs. 7c and 7d. The second mode based on the *monthly* mean data resembles the first mode using the *seasonal* mean data (Figs. 7a,b). The squared covariance explained by the first and the second monthly mean SVD modes is 29.5% and 26.1%, respectively. The first two SVD time series are correlated with the 500-mb geopotential height over the Pacific–North American region, with lags and leads of up to 2 months. Figure 13 illustrates the correlation between the SST time series of the first SVD mode and the 500-mb height, with the height field leading by (a) 2 months, (b) 1 month, and (c) 0 months, and lagging by (d) 1 month and (e) 2 months. There are significant correlations when the 500-mb height leads the SST by 1 month for the North Pacific mode (Fig. 13b), whereas the correlation is negligible when the 500-mb height lags the SST by 1 month (Fig. 13d). This asymmetry in correlation with respect to the lags and leads is consistent with Davis (1976) and suggests a strong atmospheric forcing to the North Pacific SST. However, over most of the North Pacific and North American region,

---

←

FIG. 11. The geostrophic wind composites calculated from the 500-mb height field. Shown are wind vector (arrows) and magnitude (contours) composites based on (a) three wet years, 1951, 1952, and 1958; (b) three dry years, 1976, 1983, and 1988; and (c) (a) − (b). Contour intervals are 5 m s⁻¹ in (a) and (b), and 2.5 m s⁻¹ in (c). Arrow size is indicated below the bottom diagram.

(b) Corr(SLP, Precip Mode 1)

(d) Corr(SLP, Precip Mode 2)

(a) Corr(SLP, SST Mode 1)
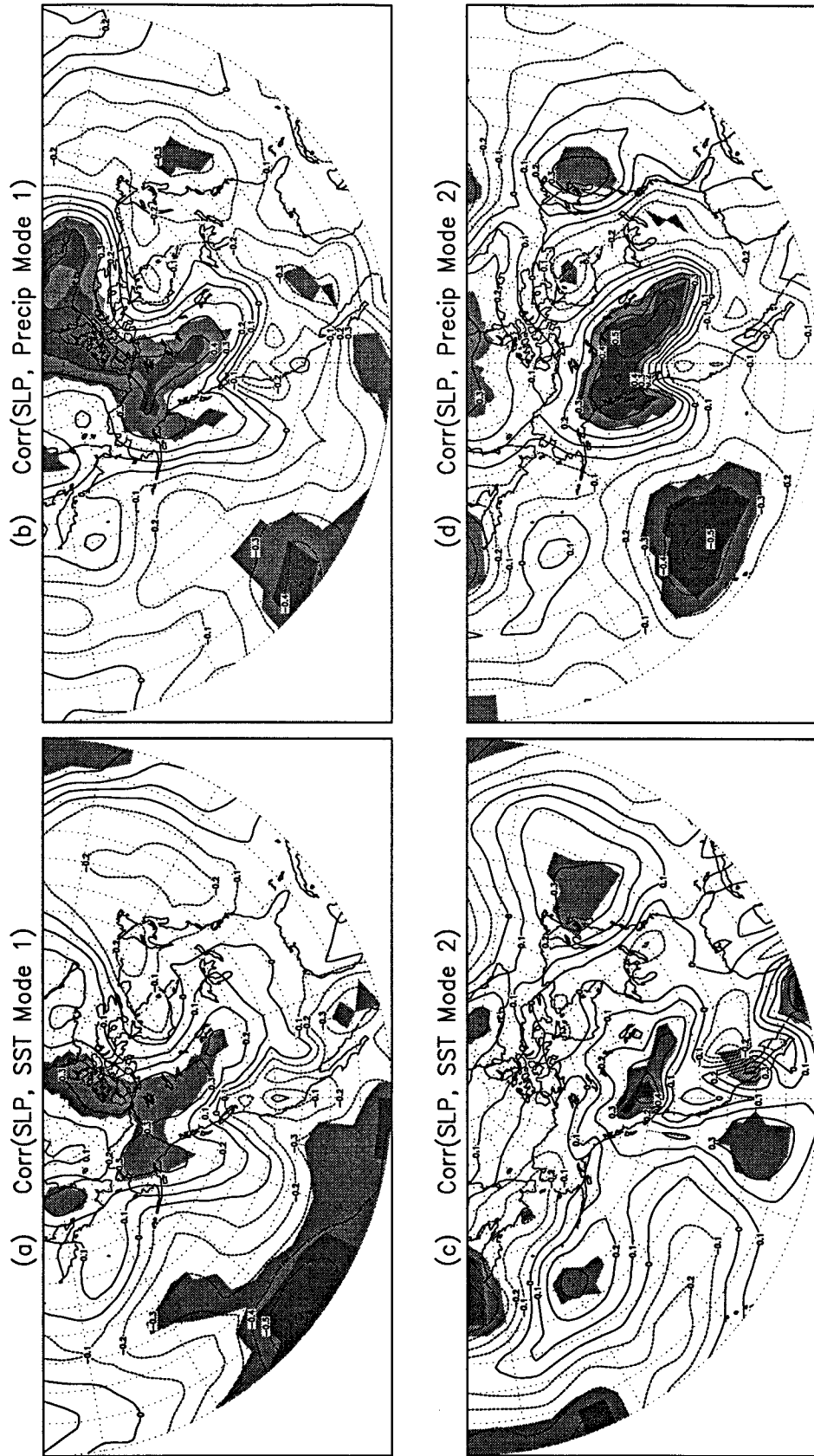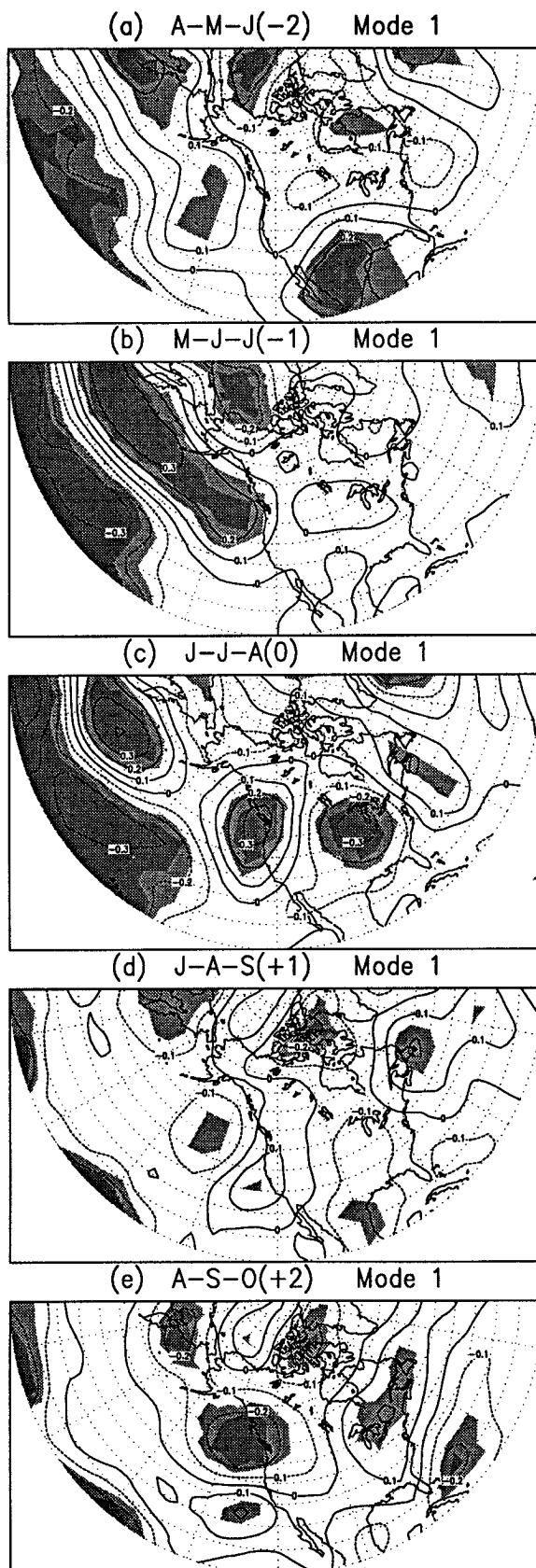
(c) Corr(SLP, SST Mode 2)

FIG. 12. Correlation coefficient of the sea level pressure with (a) mode 1 SST time series, (b) mode 1 precipitation time series, (c) mode 2 SST time series, and (d) mode 2 precipitation time series. Contour interval is 0.1, and negative contours are dashed. Shadings are the same as in Fig. 6.

(a) A−M−J(−2) Mode 1

(b) M−J−J(−1) Mode 1

(c) J−J−A(0) Mode 1

(d) J−A−S(+1) Mode 1

(e) A−S−O(+2) Mode 1

the simultaneous correlation (Fig. 13c) is stronger than that at 1-month lead (Fig. 13b). The spatial pattern is also significantly different between simultaneous and 1-month lead correlation.

The slightly stronger contemporaneous correlation (Fig. 13b), compared with the correlation at 1-month lead time (Fig. 13b), suggests that there may be feedbacks from the North Pacific SST to the atmospheric circulation. The typical timescale for the atmosphere to respond to changes in SST is about 1 week; thus, possible feedbacks of the SST will be contained in the simultaneous correlation, not in lag correlations. One possible feedback of the North Pacific SST is the maintenance of the stronger (weaker) Pacific jet by the cold (warm) SST anomalies. The cold (warm) SST helps to intensify (reduce) the meridional surface temperature gradient south of the SST anomaly. Through turbulent mixing, the stronger (weaker) meridional SST gradient will translate into a larger (smaller) meridional gradient in the surface air temperature. Since the climatological position of the Pacific jet in the summer is located at about 40°N, the larger (smaller) meridional surface temperature gradient may help to maintain a stronger (weaker) Pacific jet. The dry and wet composites in Fig. 11 support the notion that a stronger and narrower jet exists in dry summers and a weaker and southward-shifted jet exists in wet summers. Note, however, that these features may be a manifestation of the atmospheric forcing at 1-month lead and may not be entirely the atmospheric response to SST forcing.

One possible effect of a stronger Pacific jet is the enhanced storm activity and associated convection over the Pacific. Due to the short record of the outgoing longwave radiation (OLR) data, only 2 out of the 6 extreme years considered have OLR data available; both were characterized by dry conditions over the United States and cold SST anomalies over the North Pacific. The OLR anomalies for the summers of 1983 and 1988 are shown in Fig. 14. In both cases, negative OLR anomalies were present in the jet entrance region at about 30°N and 150°E, as well as over the exit region at 45°N and 130°W. A similar dipole pattern over the western Pacific to that in Fig. 14a was also identified in Nitta (1986) using high-cloud amount data for a 6-yr period, 1978–83. The teleconnection of this cloud pattern with the global atmospheric circulation is established in Nitta (1987). A similar wave train spanning the Pacific and North American region to that in Fig. 10c is also found

←

FIG. 13. Lag/lead correlation between 500-mb height and the SST time series of the first SVD mode between summer *monthly* (June, July, and August) mean Pacific SST and the U.S. precipitation. The fast mode is the North Pacific mode. Shown are correlations with 500-mb height leading the SST by (a) 2 months, (b) 1 month, (c) 0 months, and lagging by (f) 1 month and (g) 2 months. Contour interval is 0.1, and negative contours are dashed. Shadings are the same as in Fig. 6.

OUTGOING LONG WAVE RADIATION FLUX

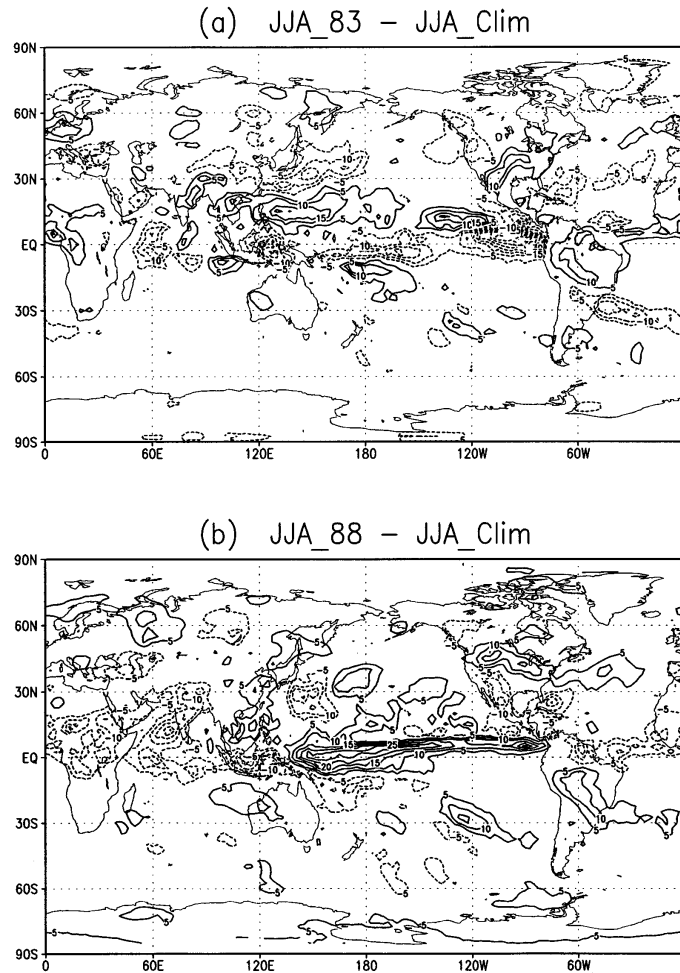### (a)   JJA_83 − JJA_Clim

(b)   JJA_88 − JJA_Clim

FIG. 14. Anomalous outgoing longwave radiation for (a) JJA 1983 and (b) JJA 1988. Data are taken from the NCEP CD-ROM published in the January 1996 issue of the *Bulletin of the American Meteorological Society* for the period 1979–94. Contour interval is 5 W m^{-2}, and negative contours are dashed. The zero contour is omitted for clarity.

in Nitta (1987) using geopotential heights at several selected pressure levels. The effect of the anomalous convection over the North Pacific on the drought circulation of the United States needs to be examined further in the future.

The first seasonal mean SVD mode between the Pacific SST and the U.S. precipitation reveals a linkage between El Niño–La Niña SST anomalies and the northern Great Plains precipitation fluctuations during summer. This linkage had been discussed in many earlier studies (Ropelewski and Halpert 1986; Trenberth et al. 1988; Trenberth and Guellimot 1996; Bunkers et al. 1996; among others). The main physical mechanism in this linkage is the change in tropical convection associated with the El Niño–La Niña conditions over the

tropical Pacific and the subsequent change in atmospheric circulation through Rossby wave dispersion from the anomalous tropical convection (Hoskins and Karoly 1983). The correlation structure in Figs. 10a and 10b supports the idea of Rossby wave propagation from the tropical central Pacific toward the North Pacific and North American region. Although the Rossby wave mechanism has proven to be essential in explaining the tropical–extratropical interactions during winter, it is not as well established for the summer. The difficulty arises mainly from the strong easterlies in the Tropics during the summer, which tend to trap the Rossby wave propagation from the Tropics to the midlatitudes. Trenberth and Branstator (1992) emphasized the importance of the atmospheric response to anomalous tropical convection

during the late spring and early summer (May and June) of 1988. The result in Fig. 9b supports the role of tropical SST anomalies in the spring on the following summer precipitation anomalies.

5. Summary

The year-to-year U.S. precipitation fluctuations in the summer are examined in this study using data from 1950–90. The amounts of precipitation vary greatly over the Great Plains area, with maximum fluctuation over the states of Kansas and Missouri. Three extremely wet and dry events are selected from the 41-yr record. The three wettest years are all found in the 1950s, and the three driest years are found after 1976, consistent with a slight decadal trend in precipitation time series. The spatial structure of the summer seasonal mean precipitation anomalies for the six extreme events is rather smooth and covers the large area of the central and eastern United States. The tropical Pacific SST associated with the extremely dry and wet events varies from one case to the other, with the 1988 dry summer being associated with a strong La Niña and the 1983 dry summer with a weak El Niño. The North Pacific SST anomaly, however, shows a consistent pattern for almost all six cases, with a cold (warm) SST over the eastern and western North Pacific, and a warm (cold) SST over the central North Pacific for the wet (dry) summers.

The precipitation index based on area-averaged precipitation over the Great Plains region shows a significant positive correlation with the eastern North Pacific and the tropical Pacific SST and a negative correlation with the central North Pacific SST. We further identified two coupled modes of variability between the U.S. precipitation and the Pacific SST using a singular value decomposition analysis. The first mode is predominantly a tropical SST mode, which is coupled with precipitation variations over the northern Great Plains, while the second mode is a midlatitude mode and shows significant structure over the North Pacific. The tropical SST mode is further shown to be related to an El Niño–La Niña event, which goes through its life cycle from the spring before the summer to the winter after the summer. During the summer, the El Niño–La Niña is under way and tends to exert influence on the atmospheric circulation over the North American region through changes in tropical convection (Trenberth et al. 1988; Trenberth and Branstator 1992). For the second mode, there is a weak indication of a tropical Pacific connection in the winter and spring before the summer. This tends to fade away quickly as the season progresses. The U.S. precipitation is mainly coupled to the midlatitude Pacific SST fluctuations in summer for the second mode. A single drought event may be a result of both the tropical and the midlatitude modes,

as was the 1988 event, or a result of the cancellation of the two, as was the 1983 summer.

Further data analysis using the 500-mb heights indicates that both the SST and precipitation variations are correlated with the 500-mb height fields over the Pacific and North American region. The height anomaly tends to place a cyclonic center over the North American region north of the maximum precipitation anomaly during wet summers. This cyclonic center is associated with a southward-shifted and enhanced jet over the United States. The sea level pressure correlations show similar features to those of the 500-mb heights but with much weaker amplitude over the land area. The anomaly centers on the sea level pressure correlation are shifted slightly eastward relative to the centers at 500 mb.

The linkage between the North Pacific SST and the U.S. precipitation is hypothesized to be through the atmospheric circulation, rather than direct moisture transport from the Pacific. The change in atmospheric circulation can be linked to both changes in moisture transport from the Gulf of Mexico and the frequency of storm activity passing through the United States. The North Pacific SST is strongly forced by the atmospheric circulation pattern over the North Pacific 1 month earlier. Enhanced westerlies at 40°N in the Pacific tend to force a cold SST anomaly across the North Pacific a month later. This cold SST anomaly may feed back onto the atmospheric circulation through a tighter meridional temperature gradient, which maintains a stronger jet. The change in convection associated with the stronger Pacific storm track may lead to further circulation changes over the Pacific and North American region, as shown in Figs. 10c and 10d.

The tropical Pacific SST exerts an influence on the atmospheric circulation through the anomalous tropical convection. A wave train is established as a result of the Rossby wave dispersion, which places a low pressure center over northern Canada in wet summers. The southern edge of the low pressure center corresponds to southward-shifted and enhanced westerlies. Since storm track changes are shown to be associated with the change in jet strength and location, a southward-shifted and intensified jet over the United States in wet summers will lead to more storm activity farther to the south, which can easily tap the moisture source from the Gulf of Mexico.

Various interactions within the atmosphere–land–ocean system inevitably complicate any explanation of the observed relationship. The U.S. precipitation itself is a very complicated quantity, which involves many different spatial and temporal scales. For example, during a flood year, the excessive precipitation may come from an airmass thunderstorm, a mesoscale convective complex, or fronts and synoptic-scale systems. How the atmospheric circulation influences each of these systems and the extent to which they may be predictable needs to be studied further. The moisture source for the United

States may differ from local evaporation to advection of moisture from a remote region. If local evaporation is important, soil moisture feedback becomes an important factor. Finally, the sequence of the drought and flood development for each of the events needs to be examined more carefully. Given the time evolution of the tropical SST shown in Fig. 9, it is important to understand the role of springtime SST anomalies on and the possible preconditioning of the summer drought and flood. All of these uncertainties need to be determined using more accurate observations and careful analysis. General circulation model experiments with fixed tropical and midlatitude SSTs in northern summer conditions will certainly be helpful in understanding the observed relationship as well.

REFERENCES

Alexander, M. A., 1992a: Midlatitude atmosphere–ocean interaction during El Niño. Part I: The North Pacific Ocean. *J. Climate,* **5,** 944–958.

——, 1992b: Midlatitude atmosphere–ocean interaction during El Niño. Part II: The Northern Hemisphere atmosphere. *J. Climate,* **5,** 959–972.

Atlas, R., N. Wolfson, and J. Terry, 1993: The effect of SST and soil moisture anomalies on GLA model simulations of the 1988 U.S. summer drought. *J. Climate,* **6,** 2034–2048.

Blackmon, M. L., G. W. Branstator, G. T. Bates, and J. E. Geisler, 1987: An analysis of equatorial Pacific sea surface temperature anomaly experiments in general circulation models with and without mountains. *J. Atmos. Sci.,* **44,** 1828–1844.

Branstator, G. W., 1995: Organization of storm track anomalies by recurring low-frequency circulation anomalies. *J. Atmos. Sci.,* **52,** 207–226.

Bretherton, C. S., C. Smith, and J. M. Wallace, 1992: An intercomparison of methods for finding coupled patterns in climate data. *J. Climate,* **5,** 541–560.

Bunkers, M. J., J. R. Miller Jr., and A. T. DeGaetano, 1996: An examination of El Niño–La Niña-related precipitation and temperature anomalies across the northern plains. *J. Climate,* **9,** 147–160.

Chang, F.-C., and J. M. Wallace, 1987: Meteorological conditions during heat waves and droughts in the United States Great Plains. *Mon. Wea. Rev.,* **115,** 1253–1269.

Davis, R. E., 1976: Predictability of sea surface temperature and sea level pressure anomalies over the North Pacific Ocean. *J. Phys. Oceanogr.,* **6,** 249–266.

Deser, C., and M. L. Blackmon, 1995: On the relationship between tropical and North Pacific sea surface temperature variations. *J. Climate,* **8,** 1677–1680.

Graham, N. E., 1994: Decadal-scale climate variability in the tropical and North Pacific during the 1970s and 1980s: Observations and model results. *Climate Dyn.,* **10,** 135–162.

Groisman, P. Ya., and D. R. Legates, 1994: The accuracy of United States precipitation data. *Bull. Amer. Meteor. Soc.,* **75,** 215–227.

Held, I. M., S. W. Lyons, and S. Nigam, 1989: Transients and the extratropical response to El Niño. *J. Atmos. Sci.,* **46,** 163–174.

Hoerling, M. P., and M. Ting, 1994: Organization of extratropical transients during El Niño. *J. Climate,* **7,** 745–766.

Horel, J. D., and J. M. Wallace, 1981: Planetary-scale atmospheric phenomena associated with the Southern Oscillation. *Mon Wea. Rev.,* **109,** 813–829.

Hoskins, B. J., and D. J. Karoly, 1981: The steady linear response of a spherical atmosphere to thermal and orographic forcing. *J. Atmos. Sci.,* **38,** 1179–1196.

Kalnay, E., and Coauthors, 1996: The NCEP/NCAR 40-year reanalysis project. *Bull. Amer. Meteor. Soc.,* **77,** 437–471.

Kushnir, Y., and N.-C. Lau, 1992: The general circulation model response to a North Pacific SST anomaly: Dependence on time scale and pattern polarity. *J. Climate,* **5,** 271–283.

——, and I. M. Held, 1996: Equilibrium atmospheric response to North Atlantic SST anomalies, *J. Climate,* **9,** 1208–1220.

Lanzante, J. R., 1984: A rotated eigenanalysis of the correlation between 700-mb heights and sea surface temperature in the Pacific and Atlantic. *Mon. Wea. Rev.,* **112,** 2270–2280.

Lau, N.-C., 1985: Modeling the seasonal dependence of the atmospheric response to observed El Niños in 1962–76. *Mon. Wea. Rev.,* **113,** 1970–1996.

——, 1988: Variability of the observed midlatitude storm tracks in relation to low-frequency changes in the circulation patterns. *J. Atmos. Sci.,* **45,** 2718–2743.

——, and M. J. Nath, 1994: A modeling study of the relative roles of tropical and extratropical SST anomalies in the variability of the global atmosphere–ocean system. *J. Climate,* **7,** 1184–1207.

Lyon, B., and R. M. Dole, 1995: A diagnostic comparison of the 1980 and 1988 U.S. summer heat wave–droughts. *J. Climate,* **8,** 1658–1676.

Madden, R. A., and J. Williams, 1978: The correlation between temperature and precipitation in the United States and Europe. *Mon. Wea. Rev.,* **106,** 142–147.

Mo, K. C., J. R. Zimmerman, E. Kalnay, and M. Kanamitsu, 1991: A GCM study of the 1988 United States drought. *Mon. Wea. Rev.,* **119,** 1512–1532.

——, J. Nogues-Paegle, and J. Paegle, 1995: Physical mechanisms of the 1993 summer floods. *J. Atmos. Sci.,* **52,** 879–895.

Namias, J., 1982: Anatomy of Great Plains protracted heat waves (especially the 1980 U.S. summer drought). *Mon. Wea. Rev.,* **110,** 824–838.

——, 1983: Some causes of United States drought. *J. Climate Appl. Meteor.,* **22,** 30–39.

——, 1991: Spring and summer 1988 drought over the contiguous United States—Causes and prediction. *J. Climate,* **4,** 54–65.

NOAA 1988: Climate Diagnostics Bulletin 88/6, 88/7, 88/8.

——, 1993: Climate Diagnostics Bulletin 93/6, 93/7, 93/8.

Newman, M., and P. Sardeshmukh, 1995: A caveat concerning singular value decomposition. *J Climate,* **8,** 352–360.

Nitta, T., 1986: Long-term variations of cloud amount in the western Pacific region. *J. Meteor. Soc. Japan,* **64,** 373–390.

——, 1987: Convective activities in the tropical western Pacific and their impact on the Northern Hemisphere summer circulation. *J. Meteor. Soc. Japan,* **65,** 373–390.

Peng, S., L. A. Mysak, H. Ritchie, J. Derome, and B. Dugas, 1995: The difference between early and midwinter atmospheric re-

sponses to sea surface temperature anomalies in the northwest Atlantic. *J. Climate,* **8,** 137–157.

Ropelewski, C. F., and M. S. Halpert, 1986: North American precipitation and temperature patterns associated with the El Niño/Southern Oscillation (ENSO). *Mon. Wea. Rev.,* **114,** 2352–2362.

Smith, T. M., R. W. Reynolds, R. E. Livezey, and D. C. Stokes, 1996: Reconstruction of historical sea surface temperatures using empirical orthogonal functions. *J. Climate,* **9,** 1403–1420.

Ting, M., 1991: The stationary wave response to a midlatitude SST anomaly in an idealized GCM. *J. Atmos. Sci.,* **48,** 1249–1275.

——, and M. P. Hoerling, 1993: Dynamics of stationary wave anomalies during the 1986/87 El Niño. *Climate Dyn.,* **9,** 147–164.

Trenberth, K. E., and G. W. Branstator, 1992: Issues in establishing causes of the 1988 drought over North America. *J. Climate,* **5,** 159–172.

——, and J. W. Hurrell, 1994: Decadal atmospheric–ocean variations in the Pacific. *Climate Dyn.,* **9,** 303–319.

——, and C. J. Guillemot, 1996: Physical processes involved in the 1988 drought and 1993 floods in North America. *J. Climate,* **9,** 1288–1298.

——, G. W. Branstator, and P. A. Arkin, 1988: Origins of the 1988 North American drought. *Science,* **242,** 1640–1645.

Wallace, J. M., and Q.-R. Jiang, 1987: On the observed structure of the interannual variability of the atmosphere/ocean climate system. *Atmospheric and Oceanic Variability,* H. Cattle, Ed., Royal Meteorological Society, 17–43.

——, C. Smith, and Q.-R. Jiang, 1990: Spatial patterns of atmosphere–ocean interaction in the northern winter. *J. Climate,* **3,** 990–998.

——, ——, and C. S. Bretherton, 1992: Singular value decomposition of wintertime sea surface temperature and 500-mb height anomalies. *J. Climate,* **5,** 561–576.

Walsh, J. E., and M. B. Richman, 1981: Seasonality in the associations between surface temperatures over the United States and the North Pacific Ocean. *Mon. Wea. Rev.,* **109,** 767–783.

Zhao, W., and M. A. K. Khalil, 1993: The relationship between precipitation and temperature over the contiguous United States. *J. Climate,* **6,** 1232–1236.